



# Performance comparison of two low-CO<sub>2</sub> emission solar/methanol hybrid combined cycle power systems



Yuanyuan Li<sup>a</sup>, Na Zhang<sup>b,\*</sup>, Noam Lior<sup>c</sup>

<sup>a</sup>Key Laboratory of Condition Monitoring and Control for Power Plant Equipment (North China Electric Power University), Ministry of Education, Beijing 102206, China

<sup>b</sup>Institute of Engineering Thermophysics, Chinese Academy of Sciences, Beijing 100190, China

<sup>c</sup>Department of Mechanical Engineering and Applied Mechanics, University of Pennsylvania, Philadelphia, PA 19104-6315, USA

## HIGHLIGHTS

- Two novel solar hybrid combined cycle systems have been proposed and analyzed.
- The power systems integrate solar-driven thermo-chemical conversion and CO<sub>2</sub> capture.
- Exergy efficiency of about 55% and specific CO<sub>2</sub> emissions of 34 g/kW h are predicted.
- Systems CO<sub>2</sub> emissions are 36.8% lower compared to a combined cycle with CO<sub>2</sub> capture.
- The fossil fuel demand is ~30% lower with a solar share of ~20%.

## ARTICLE INFO

### Article history:

Received 29 December 2014

Received in revised form 8 June 2015

Accepted 17 June 2015

### Keywords:

Hybrid power systems

Low/middle temperature solar heat

Methanol conversion to syngas

Thermo-chemical integration

Low CO<sub>2</sub> emission

Pre-combustion decarbonization

## ABSTRACT

Two novel hybrid combined cycle power systems that use solar heat and methanol, and integrate CO<sub>2</sub> capture, are proposed and analyzed, one based on solar-driven methanol decomposition and the other on solar-driven methanol reforming. The high methanol conversion rates at relatively low temperatures offer the advantage of using the solar heat at only 200–300 °C to drive the syngas production by endothermic methanol conversions and its conversion to chemical energy. Pre-combustion decarbonization is employed to produce CO<sub>2</sub>-free fuel from the fully converted syngas, which is then burned to produce heat at the high temperature for power generation in the proposed advanced combined cycle systems. To improve efficiency, the systems' configurations were based on the principle of cascade use of multiple heat sources of different temperatures. The thermodynamic performance of the hybrid power systems at its design point is simulated and evaluated. The results show that the hybrid systems can attain an exergy efficiency of about 55%, and specific CO<sub>2</sub> emissions as low as 34 g/kW h. Compared to a gas/steam combined cycle with flue gas CO<sub>2</sub> capture, the proposed solar-assisted system CO<sub>2</sub> emissions are 36.8% lower, and a fossil fuel saving ratio of ~30% is achievable with a solar thermal share of ~20%. The system integration predicts high efficiency conversion of solar heat and low-energy-penalty CO<sub>2</sub> capture, with the additional advantage that solar heat is at relatively low temperature where its collection is cheaper and simpler. The systems' components are robust and in common use, and the proposed hybridization approach can be also used with similar benefits by replacing the solar heat input with other low heat sources, and the system integration achieves the dual-purpose of clean use of fossil fuel and high-efficiency conversion of solar heat at the same time.

© 2015 Elsevier Ltd. All rights reserved.

## 1. Introduction

The hybrid power system proposed in this paper has two energy input sources: methanol and solar heat. Methanol is considered to be a fuel alternative in both transportation and power generation

sectors and is already used in that way to limited extent. Being liquid at atmospheric conditions, it is easier and cheaper to transport and store than natural gas. Methanol production on large scale is generally based on the chemical synthesis of syngas mostly produced either from natural gas reforming or coal gasification. The abundance of coal in China makes coal gasification especially suitable for China's needs. The integration of a coal gasifier with a combined cycle and methanol synthesis, "coal based poly-generation", provides a promising technology for power generation and

\* Corresponding author. Tel.: +86 10 82543030; fax: +86 10 82543151.

E-mail address: [zhangna@iet.cn](mailto:zhangna@iet.cn) (N. Zhang).

**Nomenclature**

$DNI$	direct solar radiation, $W/m^2$	$\eta_e$	system exergy efficiency, %
$E$	exergy, $kJ/mol-CH_3OH$	$\eta_{sol}$	net solar-to-electricity efficiency, %
$LHV$	methanol low heating value input, $kJ/kg$	$\eta_{th}$	system thermal efficiency, %
$m$	mass flow rate, $kg/s$		
$P$	pressure, bar	<i>Subscripts and superscripts</i>	
$Q$	heat, $kJ/mol-CH_3OH$	$f$	fossil fuel
$R_{wm}$	water-to-methanol molar ratio	$g$	gas
$SR_f$	fossil fuel saving ratio	$p$	primary energy
$T$	temperature, K	$ref$	reference system
$t$	temperature, $^{\circ}C$	$rad$	radiation
$W_{net}$	net power output, $kJ/mol-CH_3OH$	$sol$	absorbed solar heat
$X_{sol}$	solar thermal share	$0$	ambient state
<i>Greek symbols</i>			
$\eta_{col}$	solar collector efficiency, %		

methanol production from coal. For example, Gao et al. [1,2] analyzed and compared different poly-generation systems and concluded that such poly-generation has a potential of energy saving by 4–8% when compared with the separate production of power and methanol.

The other energy input is solar heat, effective for reducing emissions and for saving depletable fuel. The solar heat-to-power conversion efficiency in solar-only thermal power generation systems is generally low when the heat input is at low solar energy collection temperatures, e.g., the efficiency of Rankine cycle systems using organic working fluids with 100–200  $^{\circ}C$  top temperatures is generally around 10%. Raising that temperature by increasingly concentrating solar collectors raises, however, system cost and complexity. Furthermore, the transient nature of solar energy typically requires the use of costly energy storage.

In an attempt to alleviate these problems, hybrid solar/fossil systems were proposed, analyzed, and some built, in which both solar heat and fossil fuel are added in a temperature cascade way to take advantage of their costs at different temperature levels. They were shown to have a significant thermo-economic advantage over solar-only ones: an early example is the “SSPRE” (Solar Steam Powered Rankine Engine) hybrid system proposed by Lior and co-workers [3–5]. In SSPRE, solar heat at temperatures around  $\sim 100^{\circ}C$  is produced by non-concentrating (flat-plate, evacuated, stationary) simple solar collectors at relatively low cost, to provide 80% of the total system input for steam generation, with the remaining 20% of the heat demand supplied from fossil fuel for superheating the steam up to  $\sim 600^{\circ}C$ . SSPRE was shown to double the cycle efficiency, to  $\sim 18\%$ , when compared with the solar-only heat input at  $100^{\circ}C$ . Comparing this hybrid with a modern steam cycle that uses only fossil fuel at 45% efficiency, SSPRE thus reduces the fossil fuel consumption and associated  $CO_2$  emissions by half. Another example is the Solar Aide Power Generation (SAPG) system, in which solar heat is used to replace steam extraction from the turbine for feedwater heating in a regenerative Rankine plant [6–8]. With the same fossil fuel input, this hybrid cycle was predicted to achieve higher power output, by up to 30%, because of the resulting increase in the turbine working fluid mass flow rate.

Another hybridization approach which involves thermochemical integration, also employed in our proposed systems, is to use the solar heat as the process heat for driving the endothermic chemical reactions of a hydrocarbon toward the production of storable and transportable fuels. In this way, solar heat is converted into and stored as the upgraded “solar” fuel chemical energy. The heat value of such solar-produced fuel is higher than that of the hydrocarbon reactants by an amount equal to the enthalpy change

of the solar-driven reaction. A very desirable aspect of this process is that such fuels have a very high energy density and thus relatively, need small volume and are easily transportable to other locations by using conventional technology and systems. To ensure sufficient synthetic fuel supply, its solar assisted production can be processed separately at the most suitable site, and by more than a single solar unit, choosing as many solar units as needed to match the solar input required for the power block. Another advantage of this approach is that the power generation cycle can run using conventional fuel from other sources when solar heat is unavailable.

A brief review of past studies on power generation systems that incorporate solar energy use for thermochemical conversion of hydrocarbons follows, to contrast this study and show its new contribution to the state of knowledge. Most of the past studies focused on the use of concentrated solar heat at high temperatures (usually above 1000 K) for thermochemical conversion to chemical fuels [9,10]. These processes included thermal dissociation of  $H_2O$  (2000–2500 K), solar decomposition of fossil fuels, solar reforming of fossil fuels and solar gasification of coal (1000–1500 K). A solar methane reforming process ( $>1000^{\circ}C$ ) integrated with power generation (300  $kW_e$ , SOLASYA) using the produced solar fuel in a combined cycle system was proposed, analyzed and designed by Tamme et al. [11], predicting fuel savings of up to 25%. Bianchini et al. [12] studied the use of heat generated by a solar parabolic concentrator at  $600^{\circ}C$  for reforming natural gas for power generation with a steam-injected gas turbine power plant fed by a mixture of natural gas and the solar-heat-generated syngas (mainly composed of hydrogen and water steam). Compared to conventional steam injection gas turbine power plant, this hybrid system was predicted to reach up to 20% natural gas saving when the GT is fed only by the solar syngas, which allows high gas turbine performance and low  $NO_x$  and  $CO_2$  emissions.

To avoid the high cost and low efficiency caused by high temperature solar heat collection, and moreover, to allow the low/mid temperature solar heat to achieve its high-efficiency heat-to-power conversion, many past studies were about effective ways of thermochemical integration with low/mid temperature solar heat. Methane and methanol were commonly used for this purpose. For instance, Zhang and Lior proposed a solar-assisted chemically recuperated gas turbine system (SOLRGT) with indirect solar heat upgrading [13]. Solar heat collected at  $\sim 220^{\circ}C$  is used to generate steam for methane reforming, thus the solar heat is first transformed into vapor latent heat, and then converted to the produced syngas chemical energy via the reforming reaction. The upgraded solar fuel (syngas) is then burned in a high-efficiency power system. It was predicted that a 20–30% fossil fuel saving

ratio can be achieved compared with a conventional chemically recuperated gas turbine system (CRGT) without solar heat contribution. Li et al. [14] proposed and analyzed a hybrid system (LEHSOLCC) that incorporates solar-driven methane/steam membrane reforming. The reformer is integrated with a hydrogen separation membrane, enabling continuous removal of hydrogen from the retentate (reaction) zone, and thus shifting the reaction to the product side. The impermeable CO<sub>2</sub>-rich syngas is collected from the bottom of the reaction zone. Nearly complete CH<sub>4</sub> conversion can be achieved at a reforming temperature of 550 °C. A design-point performance analysis shows that the system attains a net exergy efficiency of 58% and specific CO<sub>2</sub> emissions of 25 g/kW h with 91% CO<sub>2</sub> capture ratio. A fossil fuel saving ratio of 31% is achievable with a solar thermal share of about 28%.

Methanol is endothermically reactive at relatively low-temperatures. For example, methanol-steam reforming and methanol decomposition are highly endothermic and can achieve >90% conversion into H<sub>2</sub>-rich syngas at around 250 °C. Hong and co-workers proposed a combined cycle (called Solar CC) that integrates mid-temperature solar thermal energy with methanol decomposition [15]. Rather than fueling the power block directly, the solar heat is used at low/mid temperatures to drive the endothermic methanol decomposition, thus upgraded to chemical energy of the produced syngas and attained its high efficiency conversion to power in a combined cycle system consequently. This concept mitigates both solar energy related limitations: it uses solar heat at low- to mid-level temperatures, where its collection is cheaper and simpler, and its use is for producing syngas with its high chemical storage capability that also creates physical independence of the solar block from the power system. The solar heat share of the total heat input was only 18%, the CO<sub>2</sub> was not captured, and the Solar CC system has ended up with a CO<sub>2</sub> emission of about 300 g/kW h.

Zhao and Yue [16] proposed and analyzed a conceptual advanced humid air turbine cycle (HAT). Driven by solar heat collected by a solar parabolic collector at 200–300 °C, methanol decomposition reaction is conducted to produce CO and H<sub>2</sub> enriched syngas. With the turbine inlet temperature (*TIT*) of about 1000–1300 °C, the obtained results show that the exergy efficiency of the cycle is higher by nearly 6%-points than that of the conventional HAT cycle.

Re-emphasizing, using solar heat at lower temperatures, as proposed in this study, offers more economical employment of solar energy, with the associated benefits of increased substitution of renewable energy for fuel and lower CO<sub>2</sub> emissions.

Another important advantage of the systems proposed in this study is that, as shown further below, they emit very small amounts of CO<sub>2</sub> with a very small energy efficiency penalty. Conventional techniques for CO<sub>2</sub> capture typically impose about 10%-points penalty to the system overall efficiency [17,18], so the reduction of CO<sub>2</sub> emissions would result in a commensurate reduction in overall efficiency losses due to its capture, and an important objective is to find ways to reduce these emissions by a combination of replacing some fraction of the fossil fuel by solar energy, and by efficiently integrating capture of the remaining CO<sub>2</sub> into the power system. As an example, Zhang et al. proposed a zero CO<sub>2</sub> emission solar hybrid gas turbine (ZE-SOLRGT) system employing oxy-fuel combustion [19–21].

Another family of hybrid cycles with reduced CO<sub>2</sub> emission are the solar-driven chemical-looping combustion cycles. Hong et al. proposed a solar hybrid combined cycle system incorporating methanol-fuel chemical-looping combustion and use of solar heat at about 450–500 °C for Ni-based redox and 150–300 °C for redox between FeO and Fe<sub>2</sub>O<sub>3</sub>, in which solar-driven endothermic reduction of NiO [22] or Fe<sub>2</sub>O<sub>3</sub> [23] by methanol is carried out. The CO<sub>2</sub> can be easily separated from the produced vapor by condensation,

with low energy penalty. Taking the FeO/Fe<sub>2</sub>O<sub>3</sub> based methanol-fueled chemical looping combustion as an example, a supplementary combustor is used to reach a gas turbine inlet temperature (*TIT*) of 1400 °C, and the resulting system exergy efficiency was predicted to be as high as 58.4% with a CO<sub>2</sub> separation of 55%.

In the above-reviewed solar hybrid systems that do not implement CO<sub>2</sub> capture, the system CO<sub>2</sub> emission decreases proportionally to the reduction of fossil fuel consumption, but they still produce CO<sub>2</sub> emission of 300–350 g/kW h due to the large energy input fraction from fossil fuel. Since the thermo-chemical upgrading of solar heat generates syngas from the hydrocarbon fuel, the novel systems of this study offer the best opportunity for employing pre-combustion decarbonization to the syngas and consequently for reducing CO<sub>2</sub> emission beyond what is achieved by reducing the hydrocarbon fuel just by its partial replacement with solar energy. An important innovation in this proposal and study is that, as described in more detail below (Sections 2–4), in addition to the hybridization with solar thermal energy at relatively low temperatures, the systems also employ pre-combustion decarbonization to the produced syngas, thus achieving the dual-purpose of clean use of fossil fuel and high-efficiency conversion of solar heat at the same time. The typical hybrid systems with solar thermochemical integration are summarized in Table 1, which demonstrates that the proposed systems of this study indeed have such quantitative advantages over others proposed and studied in the past.

To summarize the introduction, this paper is a proposal and analysis of two novel low-CO<sub>2</sub>-emission solar hybrid combined cycle systems based on solar-driven methanol decomposition and reforming, respectively. Pre-combustion decarbonization is also employed to the fully converted syngas that is then burned to produce heat at the high temperature for power generation in an advanced combined cycle system.

The two systems are configured with particular attention on the thermal match of internal heat recuperation with both steam generation and endothermic chemical conversion. The thermodynamic performance is simulated with ASPEN PLUS software [25], assuming steady state.

The system performance is compared with a gas-steam combined cycle system with CO<sub>2</sub> capture from its exhaust gas (CC-Post), which has no solar assistance.

As introduced above, and demonstrated in Sections 4 and 5 below, such integration of solar heat with fossil fuel thermo-chemical conversion contributes to the clean use of fossil fuel and high efficiency and relatively low cost conversion of solar heat in (1) elevation of the fuel heating value and the overall power output, (2) high efficiency conversion of solar heat, (3) low energy-penalty CO<sub>2</sub> capture integrated with energy conversion, and (4) offering the option of storing high energy density syngas instead of storing solar heat.

## 2. System configuration description

Following the thermodynamic principle of temperature-cascade use of multiple heat sources, and integration of CO<sub>2</sub> capture with energy conversion, two hybrid power systems are proposed in this study, based on solar-heat driven methanol decomposition and reforming, respectively.

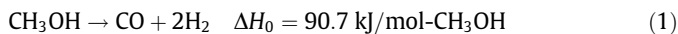
### 2.1. The proposed low CO<sub>2</sub> emission solar hybrid combined cycle system with methanol decomposition and a shift reaction (LESOLCC-DCP) system

Methanol is endothermically decomposed by heat input over a catalyst at temperatures of about 200–300 °C, and produces a mixture of H<sub>2</sub> and CO:

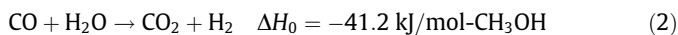
**Table 1**

Summary of the solar hybrid power generation systems, with comparison to the systems (10 and 11) proposed and analyzed in this paper.

System number and description	Solar-aided chemical reaction included	Solar heat		CO <sub>2</sub> capture	Performances	Ref.
		Temperature (°C)	Role			
1 Gas turbine cycle with methane reforming	CH <sub>4</sub> + 2H <sub>2</sub> O → CO <sub>2</sub> + 4H <sub>2</sub>	800–1000	Chemical reaction process heat	None	Fossil fuel saving: 25–40%	[11]
2 Combined cycle with methane reforming	CH <sub>4</sub> + 2H <sub>2</sub> O → CO <sub>2</sub> + 4H <sub>2</sub>	600–900	Chemical reaction process heat	None	Annual thermal efficiency: 47.6% Solar share: 9.6%	[24]
3 Steam injected gas turbine cycle with nature gas reforming	CH <sub>4</sub> + 2H <sub>2</sub> O → CO <sub>2</sub> + 4H <sub>2</sub>	600	Chemical reaction process heat	None	Natural gas saving: <20%	[12]
4 Combined cycle with solar methanol decomposition	CH <sub>3</sub> OH → CO + 2H <sub>2</sub>	200–400	Chemical reaction process heat	None	Solar to electricity efficiency: 18–35% Exergy efficiency: 50–60% CO <sub>2</sub> emission: 310 g/kW h	[15]
5 HAT cycle with methanol decomposition	CH <sub>3</sub> OH → CO + 2H <sub>2</sub>	175–210	Chemical reaction process heat	None	Solar to electricity efficiency: 25–39% Exergy efficiency: 59.2% Thermal efficiency: 53.6%	[16]
6 Chemically recuperated gas turbine cycle with solar methane reforming	CH <sub>4</sub> + 2H <sub>2</sub> O → CO <sub>2</sub> + 4H <sub>2</sub>	~220	Latent heat of reactant H <sub>2</sub> O evaporation	None	Thermal efficiency: 51.2–53.6% Solar to electricity efficiency: 25–38% Fossil fuel saving: 20%	[13]
7 Combined cycle with solar methane membrane reforming	CH <sub>4</sub> + 2H <sub>2</sub> O → CO <sub>2</sub> + 4H <sub>2</sub>	~550	Chemical reaction process heat	Membrane reaction/separation	CO <sub>2</sub> emission: 25 g/kW h Exergy efficiency: 58% Thermal efficiency: 51.6% Fossil fuel saving: 31.2% Solar share: 28.2% Solar to electricity efficiency: 36.4%	[14]
8 Zero-emission oxy-fuel combustion hybrid cycle	CH <sub>4</sub> + 2H <sub>2</sub> O → CO <sub>2</sub> + 4H <sub>2</sub>	200–400	Latent heat of reactant H <sub>2</sub> O evaporation	Oxy-fuel combustion	Thermal efficiency: 50.7% CO <sub>2</sub> capture ratio: ~100%	[19,20]
9 Hybrid methanol-fueled chemical looping combustion	(1) CH <sub>3</sub> OH + M <sub>x</sub> O <sub>y</sub> → M + CO <sub>2</sub> + H <sub>2</sub> O (2) M + O <sub>2</sub> → M <sub>x</sub> O <sub>y</sub>	150–500	Chemical reaction process heat	Chemical looping combustion	Exergy efficiency: 58.4% Solar to electricity efficiency: 22.3% CO <sub>2</sub> emission: 130 g/kW h	[22,23]
10 Combined cycle with solar methanol decomposition	CH <sub>3</sub> OH → CO + 2H <sub>2</sub>	200–250	Chemical reaction process heat	Pre-combustion	CO <sub>2</sub> emission: 33.8 g/kW h Exergy efficiency: 53.8% Thermal efficiency: 51.1% Fossil fuel saving: 27.3% Solar thermal share: 17.6% Solar to electricity efficiency: 49.2%	This paper DCP
11 Combined cycle with solar methanol reforming	CH <sub>3</sub> OH + H <sub>2</sub> O → CO <sub>2</sub> + 3H <sub>2</sub>	200–250	Chemical reaction process heat	Pre-combustion	CO <sub>2</sub> emission: 33.4 g/kW h Exergy efficiency: 55.1% Thermal efficiency: 50.9% Fossil fuel saving: 30.5% Solar thermal share: 21.5% Solar to electricity efficiency: 45%	This paper RFM



To apply pre-combustion decarbonization, an exothermic shift reaction is added that converts CO further to CO<sub>2</sub>, so that the syngas to be treated contains only H<sub>2</sub> and CO<sub>2</sub>:



Syngas composition variation with the operation parameters is shown in Fig. 1, in which both our simulation and the experimental results from [15] are plotted for comparison. It shows that the simulation and experimental results have similar trends with the variation of temperature. The experimental results show a somewhat lower reaction extent than the simulation ones, especially at temperatures below 200 °C. This difference between the simulation and experimental results is because the simulation is based on the ideal equilibrium assumption while the experimental data includes the actual irreversibilities and thermal inertia. At the temperatures of 250 °C and above, relevant to the system in this study, good agreement is achieved between them. Methanol conversion can exceed 90%, and the concentrations of CO and H<sub>2</sub> in the produced mixture are approximately 33.2% and 66.5%, respectively at around 250 °C. The temperature region of 200–300 °C fits well with that of the economical operation of parabolic trough solar collectors.

Based on the above considerations, the low CO<sub>2</sub> emission solar hybrid combined cycle system with methanol decomposition (LESOLCC-DCP) is configured as shown in Fig. 2. It is composed of

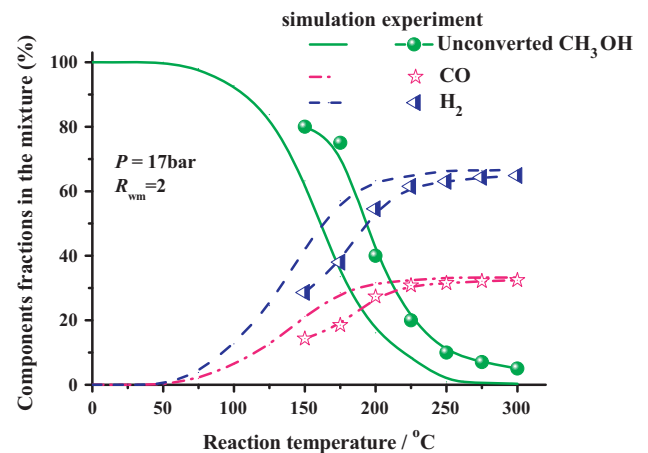
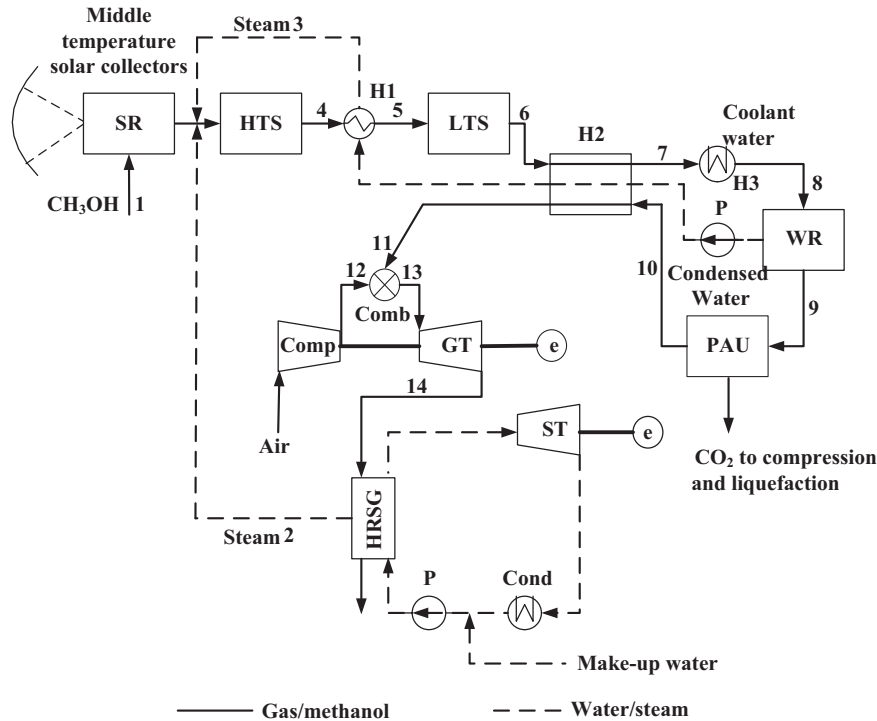


Fig. 1. Syngas composition as a function of the decomposition reaction temperature: comparison between our simulation results and experimental ones from [15].



SR: Solar reactor, HTS/LTS: High/Low temperature shift reactor, H1(H2,H3): Heat exchangers

WR: Water-removal unit, PAU: Physical absorption unit, Comp: compressor, Comb: Combustor,

GT: Gas turbine, HRSG: Heat recovery steam generator, ST: Steam turbine, Cond: Condenser, P: Pump

Fig. 2. Configuration of the low CO<sub>2</sub> emission solar hybrid combined cycle system with methanol decomposition (LESOLCC-DCP).

two main subsystems: fuel conversion/CO<sub>2</sub> capture, and power generation. The integration of CO<sub>2</sub> capture with fuel conversion is one of the new features that differentiate this system from the Solar CC cycle proposed in [15].

In the fuel conversion subsystem, solar heat delivered by parabolic trough collectors at about 250 °C provides heat for methanol evaporation and its endothermic decomposition reaction. By adding steam, the CO produced in the decomposition process is further converted to CO<sub>2</sub> in the two-stage exothermic shift reactors: the first stage is a high temperature shift reactor, 430 °C, 18.2% CO inlet concentration and 3.1% CO outlet concentration, 83% CO conversion ratio, and the second stage is a low temperature shift reactor, 235 °C, 0.5% CO outlet concentration, with an overall 97.3% CO conversion ratio in the two stages. A steam-to-carbon molar ratio >2 is selected to ensure a carbon conversion of above 94% (this value is necessary for 90% CO<sub>2</sub> removal afterwards). The addition of these shift reactions is another difference from the system studies in [15].

After being cooled down, the excess steam is condensed and removed in the water-removal unit, thus decreasing the volumetric flow of the gas to be processed, as well as increasing CO<sub>2</sub> concentration. The condensed water is pumped, and heated and evaporated by using heat recovery in the heat exchangers H1 and H2, and is then returned to the HTS inlet as a reactant. The dry syngas is then sent to the physical absorption unit for CO<sub>2</sub> removal [17,18,26]. The captured CO<sub>2</sub> is compressed to 80 bar in a four-stage compressor with intercooling, and then condensed. The liquid CO<sub>2</sub> is further pumped to 200 bar for disposal. The resulting clean fuel (~97.8% H<sub>2</sub>), warmed up by the shift products, is fed to a combined cycle for power generation.

Figure 3 shows the physical absorption unit (PAU), which consists of an absorber and a number of flash chambers in which

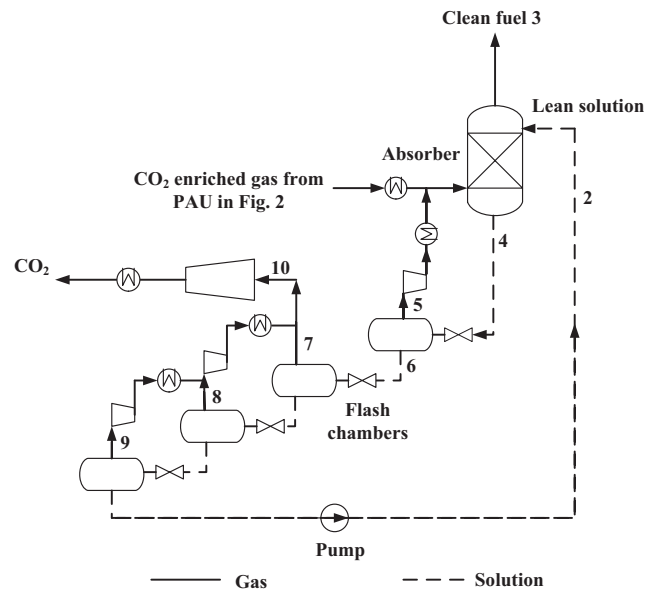


Fig. 3. Process flow diagram of physical absorption.

CO<sub>2</sub> is simply released by lowering the solution pressure (4). Gas released by the first chamber (5) includes a substantial amount of CO and H<sub>2</sub> and is thus recycled to the absorber. Multiple flashings allow a reduced compression power demand, and a large part of the CO<sub>2</sub> is released at intermediate pressures (7)–(9). From the last chamber, the lean solution (2) is pumped back to the absorber. The pressure in the last flash chamber pressure is determined by the desired CO<sub>2</sub> removal rate. A near-atmospheric chamber

pressure allows a 79.6% CO<sub>2</sub> separation. To obtain a CO<sub>2</sub> removal rate of 95%, a pressure as low as 0.25 bar would be necessary.

The internal heat recuperation, however, can produce only 40%v of the total shift-needed steam. The remainder of the needed steam (60%v of the total) is extracted from the heat recovery steam generator (HRSG, stream 2) in the power sector, rather than generated by the solar heat collection, because otherwise the large volume of steam generation would have led to a significant enlargement of the solar collector area and consequent increase in system cost, by about 36.9% and 21.1%, respectively.

The power subsystem is configured as a conventional combined cycle with a topping Brayton cycle and a bottoming tri-pressure Rankine cycle.

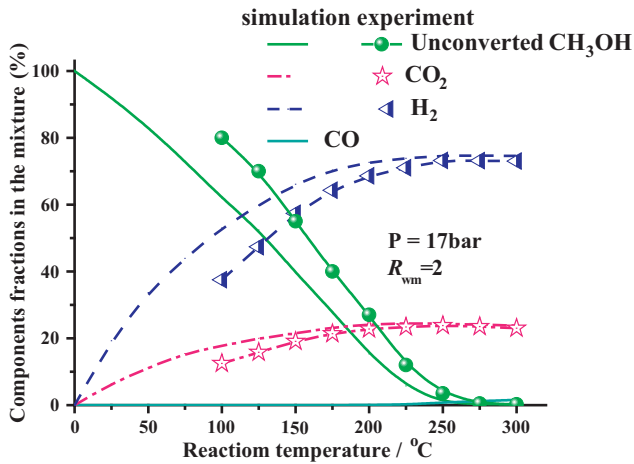
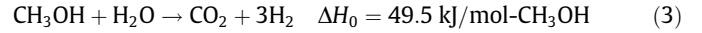


Fig. 4. Syngas composition as a function of the reforming reaction temperature: comparison between our simulation results and experimental ones from [28].

## 2.2. The proposed low CO<sub>2</sub> emission solar hybrid combined cycle system with methanol reforming (LESOLCC-RFM) system

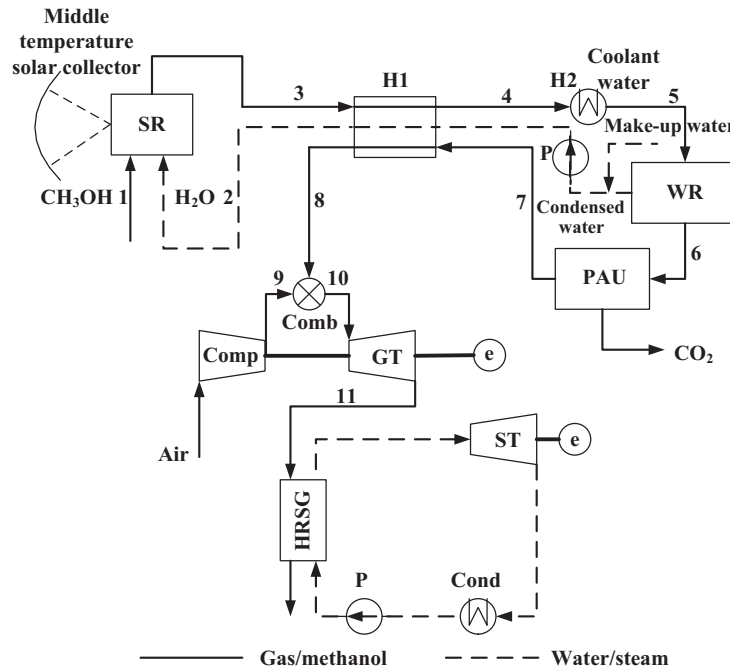
Methanol reforming is also a middle-temperature endothermic process mainly according to the endothermic reaction:



Because of the presence of steam, it produces a mixture of mainly H<sub>2</sub> and CO<sub>2</sub> [27,28], and thus is equivalent to the combination of decomposition and shift reactions. The conversion rate is also a function of temperature, pressure and the water-to-methanol molar ratio.

Figure 4 shows the variation of the syngas composition with the operation parameters, and comparison between our simulation and experimental results performed by the first authors' group [28]. It is found that methanol conversion reaches over 90% at around 250 °C. The concentrations of CO<sub>2</sub> and H<sub>2</sub> in the products are approximately 24.4% and 74.7%, and the CO concentration is negligible, well below 0.6%. The high methanol conversion rate allows the produced syngas to be processed with decarbonization prior to combustion by reduced addition of new equipment.

Figure 5 shows the flow sheet of the low CO<sub>2</sub> emission solar hybrid combined cycle system with methanol reforming (LESOLCC-RFM). Solar heat, collected at around 250 °C is applied to evaporate the reactants (liquid methanol fuel and water), and then provide heat to the endothermic reforming reaction at 17 bar. The molar ratio of water-to-liquid methanol is set to 2 to achieve CH<sub>3</sub>OH conversion higher than 95%, sufficient to allow 90% CO<sub>2</sub> removal. The presence of excess steam favors the methanol conversion, most of which is removed in the water-removal unit (WR) by condensation at a low temperature. Along with make-up water, the condensed water is pumped, heated by the reforming products and recycled back to the reformer entrance. The dry syngas is then processed with physical absorption (same as shown in



SR: Solar reactor, H1(H2): Heat exchangers, WR: Water-removal unit, PAU: Physical absorption unit, Comp: compressor, Comb: Combustor, GT: Gas turbine, ST: Steam turbine, Cond: Condenser, P: Pump HRSG: Heat recovery steam generator

Fig. 5. Configuration of the low CO<sub>2</sub> emission solar hybrid combined cycle system with methanol reforming (LESOLCC-RFM).

Fig. 3) for CO<sub>2</sub> capture. The CO<sub>2</sub> capture and compression units and the power subsystem are the same as those in the DCP system.

### 3. Simulation and validation

#### 3.1. The simulation method and main assumptions

As stated above, the cycles in the present paper are simulated using the ASPEN PLUS process simulation software [25]. The component models are based on the energy balance, mass balance, and species balance, with a default relative convergence error tolerance of 0.01%, which is the specified tolerance for all tear convergence variables. The RK-SOAVE and STEAM-TA thermodynamic models are selected for the thermal property calculations. The decomposition, shift and reforming reactors have been simulated by the Gibbs Reactor available in the ASPEN PLUS model library, which determine the equilibrium conditions by minimizing Gibbs free energy.

In the program solar block, the solar field is assumed to consist of parabolic trough concentrating solar collectors [29,30]. The CO<sub>2</sub> physical absorption in the hybrid system is based on a model developed by Lozza and Chiesa [31] using the Selexol [32] absorption medium. A conventional gas–steam combined cycle system with CO<sub>2</sub> separation from the exhaust gas (CC-Post) is also simulated for the purpose of performance comparison, in which CO<sub>2</sub> capture is accomplished by using a chemical absorption process (with monoethanolamine (MEA) [33] as the absorbent). Steam is extracted from the steam turbine for the absorbent regeneration, the corresponding energy and steam demands are calculated based on the given composition of the processed gas. The most relevant assumptions and inputs for the simulation are summarized in Table 2.

#### 3.2. The reaction model and its validation

The reactors are simulated by the Gibbs Reactor available in the ASPEN PLUS model library, which determines the equilibrium conditions by minimizing Gibbs free energy. This reaction model included in ASPEN PLUS is based on chemical equilibrium assumption and doesn't precisely reflect reality especially at temperatures below 200 °C and is therefore compared in Figs. 1 and 4 with experimental results from [15,28]. Good agreement reaches at 250 °C, which is the temperature of interest in this paper, and also at higher temperatures.

Both decomposition (producing H<sub>2</sub> and CO, the latter thus requiring the shift reactor) and reforming (producing CO<sub>2</sub> and H<sub>2</sub>) achieve methanol conversion of more than 90% at around 250 °C. This serves as the basis of the system integration.

#### 3.3. The gas turbine cooling model and power section simulation validation

High-temperature gas turbine performance is very sensitive to blade cooling requirements, and accounting for blade cooling would reduce the efficiency. These effects are included this study, by adapting and incorporating a closed-loop steam cooling (CLSC) model. The gas turbine is divided into 4 stages assuming equal enthalpy drops, and the first 2 stages are cooled. The needed coolant is extracted from the high pressure steam turbine outlet, and the remaining turbine exhaust steam is returned to the HRSG for reheating. After cooling the stationary and rotary hot components, the steam reaches the reheating temperature. It is then mixed with the reheated steam from the HRSG and introduced into the intermediate pressure steam turbine section for expansion. To analyze the global performance of the cycle under investigation, a discrete (rather than differential field) model is used because of

its computational convenience. A more detailed description of the cooling model can be found in [14], which is based on the cooled turbine model with closed loop steam cooling (CLSC) presented in a previous study [34], and its refined versions in [35,36]. Its validation was by calibration against the published performance data in [34].

To validate this steam cooling model and the power section model, a conventional gas–steam combined cycle power system was simulated using ASPEN PLUS and compared with a reference combined cycle system presented in [37]. Both of them consist of a gas topping cycle based on the MS9001H technology ( $TIT = 1427$  °C,  $\pi = 23$ ) and a tri-pressure steam bottoming cycle with the same design parameters. The thermodynamic performance comparison results show that the mass flow rate ratio of the coolant steam to the topping cycle combustion gas is 8.4%, which is 2.4% higher than that in [37]. The combined cycle specific work output and thermal efficiency are found to be 765 kJ/kg and 61.2%, respectively, higher by 1.5% and 1.8% as compared with the reference data.

## 4. System performance analysis and comparison

### 4.1. Performance criteria

Evaluation of energy efficiency in the studied systems is done here in two ways, one based on the system direct input criteria, and the other based on primary energy inputs. In the first approach, the solar energy input is expressed as the heat that was generated by the solar collectors, and the fuel energy input is the lower heat value (LHV) of the methanol. In the second approach, using the primary energy sources, the solar energy input is the insolation on the collectors, and the methanol energy is composed of the energy needed to produce it in a process appropriate to the nature of the study (here we choose its production from coal) plus the methanol LHV. It is noteworthy to re-emphasize that the direct input approach ignores the conversion efficiency of insolation to heat and the energy needed to produce the methanol.

The system direct thermal efficiency is defined as:

$$\eta_{th,d} = \frac{W_{net}}{Q_{f,d} + Q_{sol,d}} = \frac{W_{net}}{m_f \cdot LHV + Q_{sol,d}} \quad (4)$$

where  $W_{net} = W_{out} - W_m$  is the system net work output, LHV is the fuel low heating value input, which is 19917 kJ/kg, and  $Q_{sol,d}$  is the collected solar heat input to the system.  $W_{out}$  is the system gross work output;  $W_m$  is the electric work needed for pumps, compressors, fans.

The primary energy based system thermal efficiency is defined as:

$$\eta_{th,p} = \frac{W_{net}}{Q_{f,p} + Q_{sol,p}} \quad (5)$$

where  $Q_{sol,p}$  is the total solar energy incident on the solar concentrator, and

$$Q_{f,p} = m_f(LHV + e_{f,m}) \quad (6)$$

where  $e_{f,m}$  is the specific energy for manufacturing the methanol fuel, which is 1344 kJ/mol for the coal-based methanol production process [1].

In the performance evaluation based on primary energy inputs, where the system input resources involve the methanol chemical exergy and solar thermal energy, which are different in their energy qualities, exergy efficiency is more suitable than energy efficiency for the system performance evaluation. Assuming that methanol chemical exergy is approximately equal to 1.05 times its lower heating value LHV, and the solar thermal exergy

corresponds to the maximal work availability between the solar collector temperature  $T_{sol}$  and the ambient (or dead state) temperature  $T_0$ , i.e.,  $Q_{sol,d} (1 - T_0/T_{sol})$ , the definition of the system exergy efficiency based on the direct input is given as follows:

$$\eta_{e,d} = \frac{W_{net}}{E_{f,d} + Q_{sol,d}(1 - T_0/T_{sol})} = \frac{W_{net}}{1.05m_f \cdot LHV + Q_{sol,d}(1 - T_0/T_{sol})} \quad (7)$$

The contribution of the low/mid temperature level solar heat can be measured by its share based on the direct energy input:

$$X_{sol,d} = \frac{Q_{sol,d}}{Q_{f,d} + Q_{sol,d}} = \frac{Q_{sol,d}}{m_f \cdot LHV + Q_{sol,d}} \quad (8)$$

To evaluate the performance of the solar heat conversion in the proposed system, we compare it to that of a reference system with the same methanol input but without solar contribution.

The net solar-to-electricity efficiency [15] is defined as:

$$\eta_{sol} = \frac{W_{net} - W_{ref}}{Q_{sol,p}} = \frac{W_{net} - Q_f \eta_{th,ref}}{Q_{sol,p}} \quad (9)$$

where  $W_{ref} = Q_f \eta_{th,ref}$  is the net power output generated by a reference system with the same methanol input,  $Q_{sol,p}$  represents the total solar energy incident on the solar concentrator. Here, a conventional gas–steam combined cycle system with CO<sub>2</sub> separation from the exhaust gas (CC-Post) is chosen as the reference system, operating at the conditions shown in Table 2.

The fossil fuel saving level in comparison with the reference power plant, for generating the same amount of electricity, is defined as the fossil fuel saving ratio:

$$SR_f = \frac{W_{net}/\eta_{th,ref} - Q_f}{W_{net}/\eta_{th,ref}} = 1 - \frac{Q_f \cdot \eta_{th,ref}}{W_{net}} = 1 - \frac{W_{ref}}{W_{net}} \quad (10)$$

#### 4.2. Overall performance discussion and comparison

Using the computational assumptions and models given in Section 3.1, the LESOLCC-DCP, LESOLCC-RFM and CC-Post systems are simulated on the same basis of methanol input and operation conditions. The main process stream data for the two LESOLCCs are shown in Tables 3 and 4, respectively, and the thermodynamic performance of the three systems is summarized and compared in Table 5.

The reforming can be regarded as the combination of decomposition and shift reactions, provided that the operation conditions and reactant parameters (including the reaction temperature, pressure and steam/carbon molar ratio) are the same. The interference between the decomposition and shift, however, restrain each other somewhat because one is endothermic and the other is exothermic, leading to the slight lower carbon-to-CO<sub>2</sub> conversion ratio in the RFM system and a fine difference in the syngas compositions at the Water Removal (WR) inlet. In both systems, the process heat from the fuel conversions is recuperated internally; the major difference between them is in the way that solar heat is introduced and in its amounts. While the solar heat drives the endothermic methanol conversion in both systems, solar heat in the reforming

**Table 2**  
Main assumption for the simulation and calculation.

DCP&RFM	Parameters	Value	Source
Compressor	Pressure ratio	15	Ertesvåg et al. [43]
	Polytropic efficiency	89%	Ertesvåg et al. [43]
	Compressor air leakage	1%	Ertesvåg et al. [43]
Gas turbine	Inlet temperature	1308 °C	GT World [44]
	Isentropic efficiency	88%	GT World [44]
Combustor	Pressure drop (of inlet pressure)	3%	Ertesvåg et al. [43]
Heat exchanger	Minimum temperature difference	15 °C	Ertesvåg et al. [43]
	Pressure loss	3%	Ertesvåg et al. [43]
Steam turbine	HP steam pressure	111 bar	Ertesvåg et al. [43]
	RH/IP steam pressure	27 bar	Ertesvåg et al. [43]
	LP steam pressure	4 bar	Ertesvåg et al. [43]
	Condensing pressure	0.06 bar	Ertesvåg et al. [43]
HRSG	HP/RH steam temperature	570 °C	Ertesvåg et al. [43]
	Pinch-point temperature difference	15 °C	Ertesvåg et al. [43]
	Hot side pressure drop	3%	Ertesvåg et al. [43]
	Cold side pressure drop	5%	Ertesvåg et al. [43]
Pump	Minimum stack temperature	100 °C	Ertesvåg et al. [43]
	Efficiency	85%	Ertesvåg et al. [43]
Solar receiver–reactor	Solar collector temperature	~250 °C	Hong et al. [15]
	Solar collector efficiency	62%	Hong et al. [15]
	Solar receiver–reactor pressure	17 bar	Hong et al. [15]
	Solar receiver–reactor pressure loss	10%	Hong et al. [15]
	Minimum temperature difference	20 °C	Hong et al. [15]
	Water-to-methanol molar ratio	2	Liu [28]
	CO <sub>2</sub> -to-selexol mole ratio in absorbent	0.1	Lozza and Chiesa [31]
Physical absorption	Number of flash chambers	4	Lozza and Chiesa [31]
	Last chamber pressure	To obtain 95% CO <sub>2</sub> removal	Lozza and Chiesa [31]
	Number of intercoolers for CO <sub>2</sub> compressor	3	Lozza and Chiesa [31]
	CC-Post <sup>a</sup>		
Chemical absorption	CO <sub>2</sub> -to-MEA mole ratio in absorbent	0.15	Lozza and Chiesa [31]
	Minimum temperature difference at solution regenerator	10 °C	Lozza and Chiesa [31]
	Stripping pressure	1.01 bar	Lozza and Chiesa [31]
	Steam supply	3 bar	Lozza and Chiesa [31]
	Temperature difference in reboiler	5 °C	Lozza and Chiesa [31]
	Max. gas pressure drop in absorber/stripper	4/10 kPa	Lozza and Chiesa [31]
	Number of intercoolers for CO <sub>2</sub> compressor	3	Lozza and Chiesa [31]

<sup>a</sup> Parameters of combined cycle part for the CC-Post system is the same as the proposed systems.

**Table 3**  
Main stream states of the LESOLCC-DCP system (points refer to Fig. 2).

Point	$t$ (°C)	$P$ (bar)	$m$ (kg/s)	VF	Percent molar composition (%)								
					N <sub>2</sub>	O <sub>2</sub>	CH <sub>3</sub> OH	H <sub>2</sub> O	CO <sub>2</sub>	CO	H <sub>2</sub>	Ar	
1	25	18.8	32	0.0			100						
2	207.1	18	19.8	100				100					
3	207.1	18	16.2	100				100					
4	430	17.7	68	100			0.005	23.1	16.9	3.1	56.9		
5	207.5	17.6	68	100			0.005	23.1	16.9	3.1	56.9		
6	235	17.2	68	100			0.2	20.8	19.4	0.5	59.1		
7	121.6	17.1	68	90.2			0.2	20.8	19.4	0.5	59.1		
8	30	17.1	68	79.2			0.2	20.8	19.4	0.5	59.1		
9	30	17.1	49.4	100			0.2		24.4	0.7	74.7		
10	30	17.1	9.1	100			0.3		1.6	0.9	97.2		
11	220	17	9.1	100			0.3		1.6	0.9	97.2		
12	408.3	15	619.6	100	77.3	20.7		1.01	0.03				0.92
13	1308	14.7	628.6	100	72.1	12.8		13.8	0.4				0.9
14	639.2	1.05	628.6	100	72.1	12.8		13.8	0.4				0.9

**Table 4**  
Main stream states of the LESOLCC-RFM system (points refer to Fig. 5).

Point	$t$ (°C)	$P$ (bar)	$m$ (kg/s)	VF	Percent molar composition (%)								
					N <sub>2</sub>	O <sub>2</sub>	CH <sub>3</sub> OH	H <sub>2</sub> O	CO <sub>2</sub>	CO	H <sub>2</sub>	Ar	
1	25	18.8	32	0.0			100						
2	27	18.8	36	0.0				100					
3	250	17.6	68	100			0.1	20.8	19.3	0.6	59.1		
4	121	17.3	68	90.0			0.1	20.8	19.3	0.6	59.1		
5	30	17.1	68	79.2			0.1	20.8	19.3	0.6	59.1		
6	30	17.1	49.3	100			0.2		24.4	0.8	74.7		
7	30	17.1	9.1	100			0.2		1.6	1	97.2		
8	230	17	9.1	100			0.2		1.6	1	97.2		
9	408.3	15	619.8	100	77.3	20.7		1.01	0.03				0.92
10	1308	14.7	628.9	100	72.1	12.8		13.8	0.4				0.9
11	639.2	1.05	628.9	100	72.1	12.8		13.8	0.4				0.9

system is used also for steam generation; and in the decomposition system, the additional steam for methanol conversion is extracted from the HRSG in the power subsystem. The solar thermal shares were therefore indeed found to be different, 21.5% in the RFM system and 17.6% in the DCP one.

We conclude from Table 5 that the integration of solar heat and CO<sub>2</sub> capture with fuel conversion affects the system performance in the following ways:

(A) Augments the system power output and reduced CO<sub>2</sub> emission for the same fuel input.

The solar heat stored as the syngas chemical exergy contributes to increased power output. The RFM system with the most solar heat input has the highest power output of 439 kW/(mol/s methanol), followed by the DCP system of 419 kW, higher by 44% and 37.5%, respectively, as compared with the reference CC-Post system without solar assistance.

The significant augmentation of the power output also leads to the much higher exergy and energy efficiencies of both hybrid systems, by about 29.6% and 10.9% as compared with that of the reference CC-post system.

Partial replacement of fossil fuel with solar heat contributes not only to fossil fuel saving, but also to CO<sub>2</sub> emissions reduction for the same amount of electricity generation. The fossil fuel saving ratio is found to be 30.5% for the RFM system, and 27.3% for the DCP system. The difference comes from the different solar heat input. With the same CO<sub>2</sub> capture ratio, both hybrid systems have specific CO<sub>2</sub> emission of about 33–34 g/kW h that are much lower, by about 36%, than that of the CC-Post system.

(B) Low energy-penalty CO<sub>2</sub> capture

CO<sub>2</sub> capture is energy-consuming, typically leading to a system efficiency drop up to 10%-points [17,18]. The energy penalties evaluated by thermal efficiency drops are calculated for the three systems. The efficiency penalty is defined here as the amount by which thermal efficiency decreases for the RFM, DCP and CC-Post system when compared with the respective reference systems without CO<sub>2</sub> capture.

In the CC-Post system, chemical absorption is applied to separate CO<sub>2</sub> from the flue gases, and large gas quantities have to be treated because CO<sub>2</sub> is diluted by the nitrogen in the combustion air. Steam extraction from the bottoming cycle provides the needed heat for the absorbent regeneration. The bottoming cycle power output drops accordingly and the efficiency penalty in this system is found to be 11%-points.

In contrast, CO<sub>2</sub> capture is introduced in both of our hybrid systems at the point with the highest CO<sub>2</sub> concentration and the lowest gas flow rate. Specifically, in the RFM system, production of a syngas with high CO<sub>2</sub> concentration owing to fuel conversion with a high carbon conversion ratio is thus very favorable to energy-efficient pre-combustion decarbonization for CO<sub>2</sub> capture. The efficiency penalty for CO<sub>2</sub> capture in the RFM system was found to be only 4%-points. In the DCP system, decomposition produces CO- and H<sub>2</sub>-enriched syngas, but the shift reactors introduced increase the energy consumption, resulting in a thermal efficiency penalty of 6.6%-points.

(C) High efficiency conversion of low/mid temperature solar heat

The endothermic chemical reaction of fuel conversion enables the low/mid temperature solar heat to be integrated with thermo-chemical upgrading into the chemical exergy of the produced syngas. The chemically-stored input solar heat can thus be released as high temperature thermal heat via combustion and achieves its high efficiency with the use in the advanced power system. The solar-to-electricity efficiency, (Eq. (9)), is found to be 45% and 49% for the RFM and DCP systems, respectively, much higher than that can be attained in the solar-alone system at the same solar heat collection temperature level.

(D) Significant influence of methanol production energy consumption

As a valuable alternative fuel for transportation and power generation, methanol is, however, not available naturally. Its production on commercial scale is generally based on the chemical synthesis of syngas which is produced either from natural gas reforming or coal gasification. The specific energy consumption for a typical coal-based methanol production process is about 1344 kJ/mol [1], and the solar radiation to heat conversion efficiency is chosen to be 62% for the base case calculation. Based on the primary energy inputs, the system primary thermal efficiency (Eq. (5)) quantifies the impact of the energy consumption for methanol production and the conversion efficiency of insolation to heat. It is shown in Table 5 that the primary thermal efficiency is 28% for the RFM system and 28.8% for the DCP system, which are lower by 22–23%-points than the direct thermal efficiency of the same RFM and DCP systems, suggesting a significant influence of the methanol production energy consumption and insolation-to-heat conversion efficiency. The proposed two systems have, however, higher primary thermal efficiencies than the reference CC-post system by more than 3%-points with the same methanol input.

The specific energy consumption for methanol production may vary from 1000 kJ/mol to 1500 kJ/mol, depending on the different technologies, and its influence is further investigated as shown in Fig. 6. If the methanol production energy consumption decreases from 1460 kJ/mol to near 0, the primary thermal efficiency for both RFM and DCP systems would increase from about 18% to 46%, suggesting a potential for performance improvement along with methanol production technology progress toward higher efficiency.

Despite the significant negative influence of the methanol production energy consumption and the conversion efficiency of solar radiation to heat, we believe that the principle of cascade use of multiple energy resources and integrated CO<sub>2</sub> capture with

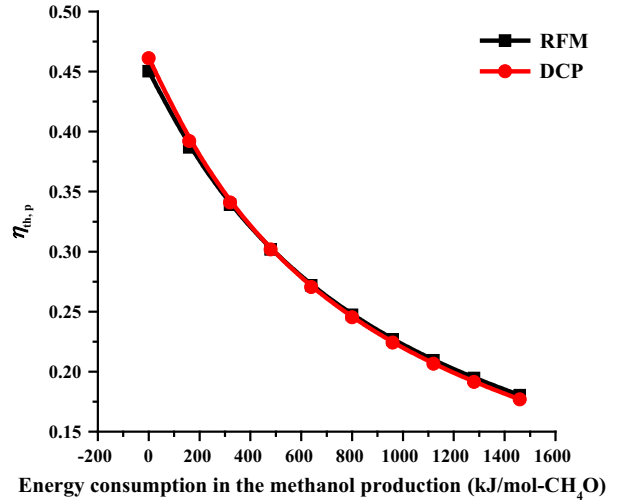


Fig. 6. Effect of energy consumption in the methanol production process on system primary thermal efficiency.

energy conversion proposed in this paper is of important value: it extends to applications beyond the methanol–solar pair and applies for system integration into hybrids in which any low temperature heat sources can be used as a process heat input for the endothermic thermochemical conversion and thus converted into chemical energy, with fossil fuel added at higher temperature to boost the efficiency.

4.3. Parametric analysis of the novel LESOLCCs systems

The water-to-methanol molar ratio  $R_{wm}$  has significant effects on system performance, by affecting fuel conversion. A sensitivity analysis was conducted to examine its effect keeping the gas turbine inlet temperature  $TIT$  and methanol input constant.

The results are summarized in Tables 6 and 7, and a comparison between the two hybrid systems is also shown in Figs. 7 and 8. It was found that RFM and DCP systems respond differently to the variation of  $R_{wm}$ . For the RFM system, solar collection provides heat for water preheating and steam generation. As more water is being introduced to the system, the solar heat thermal share consequently increases. In the DCP system, solar heat is used only for methanol evaporation and decomposition, and the solar thermal

Table 5 Systems performance comparison.

Items	LESOLCC-RFM	LESOLCC-DCP	CC-Post
Fuel direct exergy input, $E_{f,d}$ (kJ/mol-CH <sub>3</sub> OH)	716.1	716.1	716.1
Solar direct exergy input, $E_{sol,d}$ (kJ/mol-CH <sub>3</sub> OH)	79.5	61.9	–
Solar direct thermal share, $X_{sol,d}$ (%)	21.5	17.6	–
Solar-to-electricity efficiency, $\eta_{sol}$ (%)	45	49.2	–
Fossil fuel saving ratio, $SR_f$ (%)	30.5	27.3	–
CH <sub>3</sub> OH-to-CO <sub>2</sub> conversion rate, (%)	96.2	96.5	–
CO <sub>2</sub> removal rate (%)	90.8	91	90
Specific CO <sub>2</sub> emission (g/kW h)	33.4	33.8	52.8
Net power output, $W_{net}$ (kJ/mol-CH <sub>3</sub> OH)	438.6	418.7	304.5
Direct exergy efficiency, $\eta_{e,d}$ (%)	55.1	53.8	42.5
Direct thermal efficiency, $\eta_{th,d}$ (%)	50.9	51.1	45.1
Primary thermal efficiency, $\eta_{th,p}$ (%)	28	28.8	25

Table 6 Sensitivity analysis of the water-to-methanol molar ratio for LESOLCC-RFM system.

Items	Case 1	Case 2	Case 3	Case 4	Case 5
Water-to-methanol molar ratio, $R_{wm}$	0.5	1	1.5	2	2.5
Fuel direct exergy input, $E_{f,d}$ (kJ/mol-CH <sub>3</sub> OH)	716.1	716.1	716.1	716.1	716.1
Solar direct exergy input, $E_{sol,d}$ (kJ/mol-CH <sub>3</sub> OH)	59	64.4	71.7	79.5	87.9
Solar direct thermal share, $X_{sol,d}$ (%)	16.9	18.1	19.8	21.5	23.2
Solar-to-electricity efficiency, $\eta_{sol}$ (%)	65.7	56.8	50.1	45	40.6
Fossil fuel saving ratio, $SR_f$ (%)	32.3	31.1	30.7	30.5	30.4
Sequestered CO <sub>2</sub> (kg/s)	39.4	68.5	77.9	80.4	81.5
CO <sub>2</sub> removal rate (%)	44.5	77.3	88	90.8	92
Specific CO <sub>2</sub> emission (g/kW h)	196.8	81.9	43.7	33.4	29.5
Gas turbine output (kJ/mol-CH <sub>3</sub> OH)	286.3	285	284.7	284.5	284.4
Steam turbine output (kJ/mol-CH <sub>3</sub> OH)	170.1	168.1	167.5	167.3	167.2
Net power output, $W_{net}$ (kJ/mol-CH <sub>3</sub> OH)	449.9	441.8	439.3	438.6	438.2
Direct exergy efficiency, $\eta_{e,d}$ (%)	58	56.6	55.8	55.1	54.5
Direct thermal efficiency, $\eta_{th,d}$ (%)	55.3	53.5	52.1	50.9	49.8
Primary thermal efficiency, $\eta_{th,p}$ (%)	28.9	28.5	28.2	28	27.8

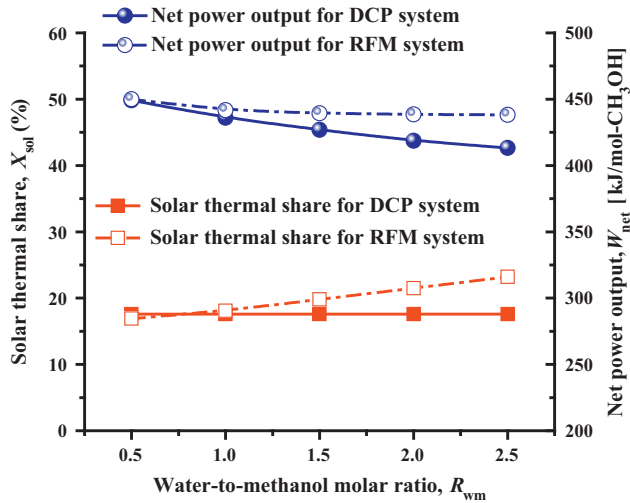


Fig. 7. Performance comparison between the two hybrid systems: LESOLCC-RFM and LESOLCC-DCP.

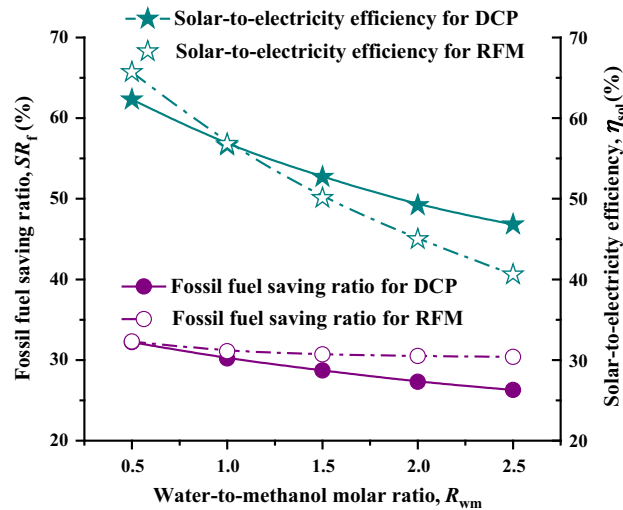


Fig. 8. Performance comparison between the two hybrid systems: LESOLCC-RFM and LESOLCC-DCP.

share remains therefore constant regardless of the steam generation rate.

Table 7  
Sensitivity analysis of the water-to-methanol molar ratio for LESOLCC-DCP system.

Items	Case 1	Case 2	Case 3	Case 4	Case 5
Water-to-methanol molar ratio, $R_{wm}$	0.5	1	1.5	2	2.5
Fuel direct exergy input, $E_{fd}$ (kJ/mol-CH <sub>3</sub> OH)	716.1	716.1	716.1	716.1	716.1
Solar direct exergy input, $E_{sol,d}$ (kJ/mol-CH <sub>3</sub> OH)	61.9	61.9	61.9	61.9	61.9
Solar direct thermal share, $X_{sol,d}$ (%)	17.6	17.6	17.6	17.6	17.6
Solar-to-electricity efficiency, $\eta_{sol}$ (%)	62.3	56.6	52.7	49.2	46.8
Fossil fuel saving ratio, $SR_f$ (%)	32.2	30.2	28.7	27.3	26.3
Sequestered CO <sub>2</sub> (kg/s)	38.6	66.5	77.2	80.7	81.7
CO <sub>2</sub> removal rate (%)	43.6	75.1	87.2	91	92.3
Specific CO <sub>2</sub> emission (g/kW h)	200	91.1	47.8	33.8	28.8
Gas turbine output (kJ/mol-CH <sub>3</sub> OH)	289.9	287.2	286	285.5	285.4
Steam turbine output (kJ/mol-CH <sub>3</sub> OH)	165.6	159.8	153.7	146.5	141.2
Net power output, $W_{net}$ (kJ/mol-CH <sub>3</sub> OH)	449.1	436	426.9	418.7	413.2
Direct exergy efficiency, $\eta_{e,d}$ (%)	57.7	56	54.9	53.8	53.1
Direct thermal efficiency, $\eta_{th,d}$ (%)	54.8	53.1	52.1	51.1	50.4
Primary thermal efficiency, $\eta_{th,p}$ (%)	28.8	28.4	28.1	27.8	27.7

In both systems, higher steam input boosts methanol conversion and shift reactions, thus favoring higher efficiency CO<sub>2</sub> removal. The CO<sub>2</sub> capture ratio increases from 44% to 92% when  $R_{wm}$  is increased from 0.5 to 2.5. The increasing steam addition, however, makes no positive contribution to the system power output, because most of the steam is finally removed in the water-removal unit downstream of the reactor. The higher methanol conversion ratio and CO<sub>2</sub> removal ratio increase the final syngas heat value on the one hand, and on the other hand reduce its mass flow rate. The latter effect dominates and the result is a slight drop of the energy input to the power subsystem. To keep the gas turbine inlet temperature  $TIT$  at the same value, the compressor inlet air mass flow rate is reduced accordingly, leading to a decrease of the system power output, from 450 kW to 438 kW/(mol/s methanol) (drop by 2.7%) in the RFM system as  $R_{wm}$  is increased from 0.5 to 2.5. The reduction in power output is more significant in the DCP system because more steam is extracted from the bottoming cycle: the specific power output drops from 449 kW to 413 kW/(mol/s methanol) (by 8%) as  $R_{wm}$  is changed from 0.5 to 2.5.

To summarize, increasing the steam addition increases the system solar heat input and reduces the power output slightly in the RFM system, while in the DCP system the system solar heat input remains unchanged and the power output drops more strongly. The system efficiencies thus decrease accordingly in both systems. For example, raising  $R_{wm}$  from 0.5 to 2.5 decreases the thermal efficiency from 58% to 54.5% in the RFM system, and from 57.7% to 53% in the DCP system.

It can be concluded that higher steam addition to these hybrid systems favors CO<sub>2</sub> capture but not power generation. Consequently, as  $R_{wm}$  is increased, the solar heat input increases in the RFM system and remains the same in the DCP system, but the solar-to-electricity efficiency and the fossil fuel saving ratio drop because both are defined based on the power generation performance alone.

In this calculation, the possibility of solid carbon formation in reforming and shift reactions at low steam content has not been considered. A water-to-methanol molar ratio of 1.5–2 is suitable for avoiding carbon deposit and attain a desired CO<sub>2</sub> capture ratio of about 90% or higher.

## 5. Technical considerations

Solar driven methanol reforming and decomposition are the key technologies for the hybrid power generation systems proposed in this paper.

Both reforming and decomposition are well established technologies in the chemical industry. With proper catalysts, they take place at a reaction temperature of 200–300 °C, much lower than that required for methane conversion.

The commercially mature parabolic trough solar concentrating collectors [3] fit well with this temperature range application.

The methanol to syngas conversion is well understood from many studies that have been conducted, numerically and experimentally, on catalysts, reaction mechanism, kinetics, and development of reactors. For example, Nakagaki developed a design method for methanol reformers by examining the reaction rates with Cu–Zn catalyst and reforming performance of a tube reactor [38]. Patel established a mechanistic kinetic model for methanol steam reforming over a Cu/ZnO/Al<sub>2</sub>O<sub>3</sub> catalyst, to predict the production rates of hydrogen, carbon dioxide and carbon monoxide for different operation conditions [39]. Hou investigated the performance of a non-isothermal solar reactor for methanol decomposition, obtained the reactor performance under different radiation intensity, beam incidence angle, and feed parameters [40]. An experimental study on solar-driven methanol reforming and decomposition has been conducted in the authors' research group [41,42]. There, a 5 kW solar receiver/reactor, positioned along the focal line of a one-tracking parabolic trough collector, was developed in these studies to demonstrate the concept of solar thermal–chemical conversion and upgrading. Experiments of H<sub>2</sub> production from methanol steam reforming at around 200–300 °C and ambient pressure were conducted. Over 90% conversion of methanol was observed, and the volumetric concentration of H<sub>2</sub> in the gas product reached 66–74% with a solar flux of 580 W/m<sup>2</sup>. The thermo-chemical efficiency of solar heat to chemical energy conversion attained 30–50%. The promising results prove the feasibility of solar-driven methanol conversion. Further development in the integration of solar receiver–reactor is needed to improve the reaction stability, conversion efficiency and to reduce the thermal loss and cost.

By combining the decomposition and shift reaction into one unit, the RFM is more compact than the DCP system. Because of the different manner of solar heat introduction and steam generation, the RFM has a higher solar direct thermal share, of 21.5%, as compared with 17.6% in the DCP system. More solar input contributes to more power output by ~5% in the RFM system; it requires, at the same time, a large solar collector surface area by 28% than in the DCP system. An economic analysis is obviously needed for a more comprehensive comparison. This paper mainly focuses on the system integration concept and thermodynamic performance at the design point.

## 6. Conclusions

Taking advantage of the high conversion ratio of methanol conversion at relatively low temperature of 200–300 °C, the authors propose the use of low/mid temperature solar heat be integrated and upgraded thermo-chemically in a way that contributes to the overall energy input, increases power generation efficiency, offers the energy storage potential of the produced syngas, and integrates low-energy-penalty pre-combustion decarbonisation. All these advantages reduce the use of fossil fuel and the associated undesirable emissions.

Two such novel system configurations have been proposed, based on solar heat methanol decomposition and reforming, respectively. The main components of the systems are power generation, solar-driven methanol thermochemical reactors, and CO<sub>2</sub> sequestration subsystems. They are simulated and compared with a conventional gas-fired gas–steam combined cycle system with CO<sub>2</sub> separation from the exhaust gas (CC-Post). The system

performance analysis results show that with the same methanol input and a chosen 91% CO<sub>2</sub> capture ratio, the specific CO<sub>2</sub> emission of the proposed hybrid systems is about 33 g/kW h, 36% lower than that in the reference conventional CC-Post cycle. Solar heat input contributes to the augmentation in system power output and, by replacement of some of hydrocarbon fuel a reduction of CO<sub>2</sub> emission. A 30% fossil fuel saving ratio is achievable with a solar thermal share of about 20%, and the net solar-to-electricity efficiency, based on the gross solar radiation incident on the collector, is more than 45% higher than that of a CC-Post system with the same fuel input, which is much higher than can be attained in the solar-alone thermal power system operating at the same or even higher solar heat temperatures.

Taking into account the methanol production energy consumption and the conversion efficiency of solar radiation to heat, the system primary thermal efficiency is found to be 28% for the RFM system and 28.8% for the DCP system, which is lower by 22–23%-points than the system direct thermal efficiency. Potential exists for system performance improvement along with technology advancement for methanol production and solar heat collection.

Summarizing, the proposed systems' thermochemical upgrading of methanol by using solar heat, and integration of cascade use of multiple heat sources was shown to accomplish much cleaner use of fossil fuel, and high efficiency conversion of low/mid temperature solar heat.

## Acknowledgment

The authors gratefully acknowledge support of the National Natural Science Foundation of China (No. 51406049).

## References

- [1] Gao L, Jin H, Liu Z, Zheng D. Exergy analysis of coal-based polygeneration system for power and chemical production. *Energy* 2004;29:2359–71.
- [2] Gao L, Li H, Chen B, Jin H, Lin R, Hong H. Proposal of a natural gas-based polygeneration system for power and methanol production. *Energy* 2008;33:206–12.
- [3] Lior N, Koai K. Solar-powered/fuel-assisted Rankine cycle power and cooling system: simulation method and seasonal performance. *ASME J Sol Energy Eng* 1984;106:142–52.
- [4] Koai K, Lior N, Yeh H. Performance analysis of a solar-powered/fuel-assisted Rankine cycle with a novel 30hp turbine. *Sol Energy* 1984;32:753–64.
- [5] Lior N, Koai K. Solar-powered/fuel-assisted Rankine cycle power and cooling system: sensitivity analysis. *ASME J Sol Energy Eng* 1984;106:447–56.
- [6] Hu E, Yang Y, Nishimura A. Solar aided power generation. *Appl Energy* 2010;87:2881–5.
- [7] Yan Q, Hu E, Yang Y, Zhai R. Dynamic modelling and simulation of a solar direct steam generating system. *Int J Energy Res* 2010;34(15):1341–55.
- [8] Yan Q, Yang Y, Nishimura A, Kouzani A, Hu E. Multi-point and multi-level solar integration into conventional power plant. *Energy Fuels* 2010;24(7):3733–8.
- [9] Steinfeld A, Palumbo R. Solar thermochemical process technology. In: Meyers RA, editor. *Encyclopedia of physical science and technology*, vol. 15. Academic Press; 2001. p. 237–56.
- [10] Kodama T. High-temperature solar chemistry for converting solar heat to chemical fuels. *Prog Energy Combust* 2003;29:567–97.
- [11] Tamme R, Buck R, Epstein M, Fisher U, Sugarmen C. Solar upgrading of fuels for generation of electricity. *ASME J Sol Energy Eng* 2001;123:160–3.
- [12] Bianchini A, Pellegrini M, Saccani C. Solar steam reforming of natural gas integrated with a gas turbine power plant. *Sol Energy* 2013;96:46–55.
- [13] Zhang N, Lior N. Use of low/mid-temperature solar heat for thermochemical upgrading of energy, part I: application to a novel chemically-recuperated gas-turbine power generation (SOLRGT) system. *ASME J Eng Gas Turb Power* 2012;134 [072301-1-14].
- [14] Li Y, Zhang N, Cai R. Low CO<sub>2</sub>-emissions hybrid solar combined-cycle power system with methane membrane reforming. *Energy* 2013;58:36–44.
- [15] Hong H, Jin H, Ji J, Wang Z, Cai R. Solar thermal power cycle with integration of methanol decomposition and middle-temperature solar thermal energy. *Sol Energy* 2005;78:49–58.
- [16] Zhao H, Yue P. Performance analysis of humid air turbine cycle with solar energy for methanol decomposition. *Energy* 2011;36:2372–80.
- [17] Chiesa P, Consonni S. Shift reactors and physical absorption for low CO<sub>2</sub> emission IGCCs. *ASME J Eng Gas Turb Power* 1999;121:295–305.

- [18] Chiesa P, Consonni S, Lozza G. A comparative analysis of IGCCs with CO<sub>2</sub> sequestration. In: GHGT1999: proceedings of the 4th international conference on greenhouse gas control technologies. Interlaken, Switzerland; 1999.
- [19] Zhang N, Lior N, Luo C. Use of low/mid-temperature solar heat for thermochemical upgrading of energy, part II: a novel zero-emissions design (ZE-SOLRGT) of the solar chemically-recuperated gas-turbine power generation system (SOLRGT) guided by its exergy analysis. *ASME J Eng Gas Turb Power* 2012;134 [072302-1-8].
- [20] Luo C, Zhang N. Zero CO<sub>2</sub> emission SOLRGT power system. *Energy* 2012;45:312–23.
- [21] Li Y, Zhang N, Cai R, Yang Y. Performance analysis of a near zero CO<sub>2</sub> emission solar hybrid power generation system. *Appl Energy* 2013;112: 727–36.
- [22] Hong H, Jin H, Liu B. A novel solar-hybrid gas turbine combined cycle with inherent CO<sub>2</sub> separation using chemical-looping combustion by solar heat source. *J Sol Energy Eng* 2006;128(3):275–84.
- [23] Hong H, Han T, Jin H. A low temperature solar thermochemical power plant with CO<sub>2</sub> recovery using methanol-fueled chemical looping combustion. *J Sol Energy Eng* 2010;132(3):031002.
- [24] Sheu EJ, Mitsos A. Optimization of a hybrid solar-fossil fuel plant: Solar steam reforming of methane in a combined cycle. *Energy* 2013;51:193–202.
- [25] Aspen Plus®. Aspen Technology, Inc., Version 11.1[EB/OL]-Available at: <<http://www.aspentech.com/>> [accessed 05.01.09].
- [26] Doctor RD, Molburg JC, Thimmapuram P, Berry GF, Livengood CD, Johnson RA. Gasification combined cycle: carbon dioxide recovery, transport and disposal. *Energy Convers Manage* 1993;34:1113–20.
- [27] Agrell J, Birgersson H, Boutonnet M. Steam reforming of methanol over a Cu/ZnO/Al<sub>2</sub>O<sub>3</sub> catalyst: a kinetic analysis and strategies for suppression of CO formation. *Appl Catal A* 2002;106:249–57.
- [28] Liu Q. Novel thermochemical hydrogen production with mid-and-low temperature solar thermal energy and algebraically explicit analytical solutions of engineering thermophysics. PhD thesis. Beijing, China: Graduate School of the Chinese Academy of Sciences; 2007.
- [29] García-Rodríguez L, Gómez-Camacho C. Thermo-economic analysis of a solar multi-effect distillation plant installed at the Plataforma Solar de Almería (Spain). *Desalination* 1999;122:205–14.
- [30] Price H. Assessment of parabolic trough and power tower solar technology cost and performance forecasts. America: National Renewable Energy Laboratory; 2003. Available at: <<http://www.nrel.gov/docs/fy04osti/34440.pdf>> [accessed 30.09.10].
- [31] Lozza G, Chiesa P. Natural gas decarbonization to reduce CO<sub>2</sub> emission from combined cycles. Part 1: partial oxidation. *ASME J Eng Gas Turb Power* 2002;124:82–8.
- [32] Lampert K, Ziebig A. Comparative analysis of energy requirements of CO<sub>2</sub> removal from metallurgical fuel gases. *Energy* 2007;32:521–7.
- [33] Alie C, Backham L, Croiset E, Douglas PL. Simulation of CO<sub>2</sub> capture using MEA scrubbing: a flow-sheet decomposition method. *Energy Convers Manage* 2005;46:475–87.
- [34] Sanjay, Singh O, Prasad BN. Influence of different means of turbine blade cooling on the thermodynamic performance of combined cycle. *Appl Therm Eng* 2008;28:2315–26.
- [35] Louis JF, El-Masri MA, Hiraoko K. A comparative study of influence of different means of turbine cooling on gas turbine performance. In: GT1983: ASME international gas turbine conference (Phoenix, AZ, USA, March); 1983 [ASME Paper: 83-GT-180].
- [36] Horlock JH, Watson DT, Jones TV. Limitation on gas turbines performance imposed by large turbine cooling flows. *ASME J Eng Gas Turb Power* 2001;123:487–94.
- [37] Carcasci C, Facchini B. Comparison between two gas turbine solutions to increase combined power plant efficiency. *Energy Convers Manage* 2000;41:757–73.
- [38] Nakagaki T, Ogawa T, Murata K, Nakata Y. Development of methanol steam reformer for chemical recuperation. *ASME J Eng Gas Turb Power* 2001;123:727–33.
- [39] Patel S, Pant K. Experimental study and mechanistic kinetic modeling for selective production of hydrogen via catalytic steam reforming of methanol. *Chem Eng Sci* 2007;62:5425–35.
- [40] Hou Z, Zheng D, Jin H, Sui J. Performance analysis of non-isothermal solar reactors for methanol decomposition. *Sol Energy* 2007;81:415–23.
- [41] Liu Q, Hong H, Yuan J, Jin H, Cai R. Experimental investigation of hydrogen production integrated methanol steam reforming with middle-temperature solar thermal energy. *Appl Energy* 2009;86:155–62.
- [42] Liu Q, Jin H, Hong H, Sui J, Ji J, Dang J. Performance analysis of a mid- and low-temperature solar receiver/reactor for hydrogen production with methanol steam reforming. *Int J Energ Res* 2010;35:52–60.
- [43] Ertesvåg IS, Kvamsdal HM, Bolland O. Exergy analysis of a gas turbine combined-cycle power plant with pre-combustion CO<sub>2</sub> capture. *Energy* 2005;30:5–39.
- [44] Gas turbine world 2010 handbook. 654 Hillside Rd., Fairfield, CT 06824: Pequot Publishing Inc.; 2010.